Exploring the Impact of Scene Visual Characteristics and Adaptation Effects on Rotation Gain Perception in VR

Qi Wen Gan
yanqm21@tsinghua.org.cn
Tsinghua University
Beijing, China

Sen-Zhe Xu
xsz15@tsinghua.org.cn
Tsinghua University
Beijing, China

Fang-Lue Zhang
fanglue.zhang@vuw.ac.nz
Victoria University of Wellington
Wellington, New Zealand

Song-Hai Zhang
shz@tsinghua.edu.cn
Tsinghua University
Beijing, China

Figure 1: Our VR experimental conditions consisted of two levels of visual density (high, low), spatial sizes (landscape, room), and realism (high, low). Rows 1 and 2 demonstrate two levels of realism. Scenes with lower visual density are shown in Columns 1 and 3. Columns 2 and 4 have higher visual density. The left two columns demonstrate the lower spatial size setting (room), and the right two columns demonstrate the higher spatial size setting (landscape).

ABSTRACT

Rotation gain is a subtle manipulation technique commonly employed in Redirected Walking (RDW) methods due to its superior capability to alter a user's virtual trajectory. Previous studies have reported that the imperceptible ranges of rotation gains are influenced by various factors, resulting in different detection threshold values, which may alter RDW performance. In this study, we focus on the effects of scene visual characteristics on the rotation gain and rotation gain thresholds (RGTs), which have been less explored in this area. In our experiments, we focus on three visual characteristics: visual density, spatial size, and realism. Each characteristic is tested at two different levels, resulting in a design of eight distinct VR scenes. Through extensive statistical analysis, we find that spatial size may influence user perception of rotation gain in different virtual environments (VEs), though the effect appears to be small. No significant results of sensitivity differences were found for visual density and realism. We show that the short-term temporal effect is another predominant factor influencing user perception of rotation gain, even when users experience different visual stimuli in VEs, such as different scene visual characteristic settings in our study. This result indicates that users' adaptation effects on rotation gain can occur in as short a time as overnight intervals, rather than over weeks.

VRST 2024, October 09-11, 2024, Trier, Germany

ACM ISBN 978-1-4503-XXXX-X/18/06
https://doi.org/XXXXXXX.XXXXXXX

CCS CONCEPTS

• **Computing methodologies** → **Virtual reality**; **Perception**.

KEYWORDS

Redirected walking, gain(s) thresholds, virtual environments, perception, user experience

ACM Reference Format:
Qi Wen Gan, Sen-Zhe Xu, Fang-Lue Zhang, and Song-Hai Zhang. 2018. Exploring the Impact of Scene Visual Characteristics and Adaptation Effects on Rotation Gain Perception in VR. In *ACM VRST '24: Proceedings of the 30th ACM Symposium on Virtual Reality Software and Technology, October 09–11, 2024, Trier, Germany.* ACM, New York, NY, USA, 13 pages. https://doi.org/XXXXXXX.XXXXXXX

1 INTRODUCTION

In the domain of virtual reality (VR), real walking remains the most natural and intuitive way of navigation in a large virtual environment (VE) [5]. However, the intricate and confined physical space in which the user is situated to experience VR applications constrains the potential for unrestricted movement. To tackle this challenge, researchers have explored Redirected Walking (RDW) methods [2, 19, 30, 41, 49, 53, 63, 64, 66, 67], aiming to grant users greater freedom for physical walking when exploring virtual scenes. Among all RDW methods, rotation gain [49] has consistently been the most commonly employed subtle manipulation technique due to its superior capability in manipulating a user's virtual trajectory. It controls the ratio between user's virtual rotation $r_{virtual}$ and physical rotation $r_{physical}$: $g_r = \frac{r_{virtual}}{r_{physical}}$, $g_r \in \mathbb{R}$ at user yaw-axis movements.

In fully immersive VEs, VR users rely on optical flows [31, 61] of the scene as the main visual cue to perceive their self-motion and self-orientation when rotating in place. However, applying too large or small rotation gain creates a severe mismatch between self-motion and visual cue, inducing motion sickness [51]. Thus, to minimize this effect, some studies [11, 65] have explored the impact of different visual factors, including field of view and vignetting type, on the perception of rotation gain and its thresholds. As a result, these experiments found that the discrepancies of Low Detection Threshold (LDT) and High Detection Threshold (HDT) vary in the range of $\left[0.64, 0.88\right]$, and $\left[1.24, 1.33\right]$ respectively. The LDT and HDT are referred as rotation gain thresholds (RGTs) [65]. To date, several visual factors that influence this perception have been identified. While Paludan *et al.*[44] found that the visual density of objects had no significant effect, using a visually detailed VE as a control scene led to a marginal reduction in the user's perceived rotation speed. To address this gap, we explore user perception within VE scenes to identify potentially influential attributes.

In the field of RDW, the visual characteristics of a scene, such as realism [28, 57], visual density [44], and spatial size [26, 27] have been shown to influence detection thresholds (DTs) in translation and curvature gains. These studies suggest that manipulating visual factors within VEs can alter users' cognition in VR [36], potentially increasing their tolerance for redirection. User cognitive performance differences across VR scenes can be explained by Attention Restoration Theory [23], which posits that natural environments demand fewer cognitive resources and offer greater mental health and restorative benefits [6]. While Newman *et al.*[40] indicates that high graphical realism and specific virtual environment types can significantly impact affective responses and user perceptions, Mostajeran *et al.*[38] hypothesized that users might possess greater attentional capacities and a higher tolerance for redirection in virtual nature environments, potentially leading to higher DTs. Although their findings showed no effect of VE type on curvature gain, substantial evidence in environmental research highlights the varying cognitive perceptions of VR environments. Nonetheless, specific environmental factors, such as the angle of declination (AoD) that describes spatial size [26], and their potential impact on visual salience [1] in the context of rotation gain remain unexplored beyond the field of psychology.

Unlike translation and curvature gains, which generate translational optical flow, users must rely on their cognition of *spatial size* and perception of environmental characteristics like *realism* and *visual density* to perceive rotational flow. We hypothesize that these three visual characteristics, which are strongly tied to the visual comprehension of the scene, can significantly impact rotational flow perception. To the best of our knowledge, the effects and interactions of these three visual characteristics on the perception of rotation gain remain unknown, and RDTs may vary under different VE conditions. Exploring these three visual characteristics is crucial for optimizing virtual content and providing guidelines for RDW-related applications. Therefore, we pose the following research question: *How do the spatial size, visual density, and realism of virtual environments affect users' perception of rotation gain in VR?*

In this study, we answer our research questions by conducting comprehensive experiments. Following the methodology employed in prior studies for measuring rotation gains [44, 60, 65], we have made a within-subjects design with these three independent visual characteristics and established 2^3 experimental conditions, each consisting of two levels of visual density, spatial size, and realism. To mitigate the carry-over effects of simulator sickness [51], each user has tested on four consecutive days, with an overnight break after every two sessions. We first estimate the RGTs with standard logistic psychometric function based on users' responses to perceived speed (i.e., gain). Then, a linear mix model (LMM) [35] analysis method was utilized to verify our main research question.

Finally, we show that (i) spatial size is a potential factor that influences user perception of rotation gain, (ii) No significant results of sensitivity differences were found in visual density and realism, and (iii) a user adaptation effect, in overnight breaks has a higher influence to the RGTs compared to scene visual characteristics.

2 RELATED WORKS

2.1 Human Perception of Visual Characteristics in Virtual Environments

Human perceptions of visual characteristics in VEs are often the keys to study, together with biological and physiological sensory sensitivities [17, 32] in VR-related scenarios. In RDW, examining the effect of visual characteristics is non-trivial, as [49, 53] demonstrated that users can tolerate a certain amount of inconsistency between proprioceptive sensations and visual elements in immersive VEs. In the aspect of geometry recognition, Sun *et al.*[54] suggest that, by distorting the appearance of the geometry in VR, the user's physical movement can also be redirected. In addition, Nakamura *et al.*[39] found that eye movement trajectories tend to concentrate on specific areas such as edges and corners when humans are recognizing 3D objects in VR. Similarly, Otake *et al.*[43] suggested that speed in a hallway with few visual cues appears to be slower than in a hallway with more visual information. Vaziri *et al.*[57] also stated that the observation condition (whether the scene is viewed through the VR device or not) has a significant impact on distance perception. Still, the visual realism of the observed scene does not have a noticeable effect on perception. While [9, 61] suggest that, the optic flow fields incurred by the motion parallax can be used for manipulating the user's movements in VEs, several studies [13, 50, 52] had shown that optical flows induced were proven to be the root cause of VR simulator motion sickness (vestibular disorders).

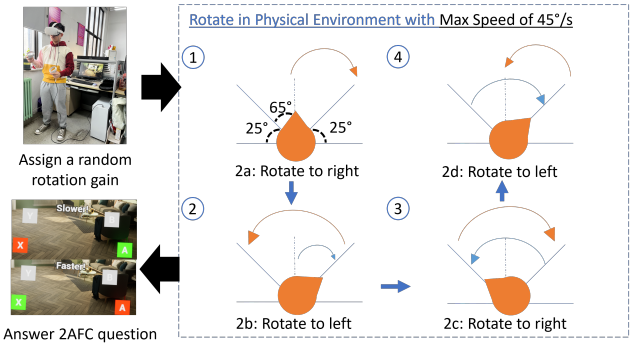

Figure 2: Standard procedure and task that each participant was required to accomplish in one experimental trial.

In psychology, previous works [40, 56] have shown that the realism of environmental presentations affects user perceptions, and the type of environment can also influence attention, potentially inhibiting or facilitating cognitive performance [38]. Several studies [37, 40] compared exposure to immersive videos of a forest and an urban environment and found lower mood disturbances, reduced simulator sickness, and a greater sense of presence in the virtual nature environment. Nevertheless, there were only a few works that studied the psychological effect of these scene visual characteristics on human locomotion, especially in RDW-related techniques.

To investigate the influence of scene visual characteristics, Kim *et al.* [26, 27] explicitly designed three different spatial sizes of the VEs, and found users perceived different translation gain thresholds in different VEs. Zhang *et al.* [67] also found that LDT and HDT for the translation gains are both closer to the point of subjective equality (PSE) value in the 360° video environment compared to the computer-generated environment. In the context of curvature detection gains measurement, Rothacher *et al.*[46] found that the human curvature gain sensitivity is correlated to the virtual visual gait and this effect was further validated in Lee's [31] recent work. With shreds of evidence, we suspect different levels of visual density, spatial size, and realism of a virtual scene can affect the user's perception of rotation speed in a fully immersive VE.

2.2 Factors that Affect Rotation Gain Thresholds in Redirected Walking

To guarantee that the applied gains are imperceptible to the user, it is imperative to measure the detection thresholds for rotation gain, i.e., rotation gain thresholds (RGTs) [65]. RGTs estimation can be accomplished by fitting a psychometric function, based on the responses from Two-Alternative Forced-Choice (2AFC) [18] questions. To date, the RGTs applied on RDW steering algorithms [2, 19, 30, 34, 49, 55, 63, 64, 66], are still heavily relied on the empirical measurements from [7, 44, 53, 60, 67]. In these measurements, the common detection thresholds for rotation gains are to be applied between 0.64 and 1.26 (lower and upper bound). Recently, Hutton et al. [21] demonstrated substantial variability in individual tolerance when using adaptive methods [16] to measure RGTs, which can complicate the validation of studies involving multiple effects. While much of the variability in RGT values is attributed to individual differences, other factors have also been identified as influential. For example, rotation speed [10], field of view (FOV) and gender [11, 65], and user VR experience [45, 47] have all been shown to affect RGTs. Additionally, differences in posture [47, 60] and gain smoothing methods [12, 20] contribute to variations in user noticeability, leading to different RGT outcomes. To address these challenges, similar studies [26, 31] have opted for the constant stimuli method [62] due to its stability and precision, particularly in complex experimental conditions. In our study, we adopted this approach to ensure consistent and reliable results.

Furthermore, in the analysis process, the interactive effect was also found to be crucial in affecting the range of RGTs [11, 45]. The repeated measures ANOVA technique is limited in accounting for only one source of random variability, such as individual differences, which can lead to less precise results. Consequently, recent research by Robb et al. [45] and Venkatakrishnan et al. [58] has recommended the use of linear mixed models (LMM) as a more appropriate method for analyzing fixed and random effects in multivariate psychophysical experiments. In addition, the preliminary results from our pilot studies suggested that the temporal variables likely influence the estimation of RGTs in a four-day experiment. Therefore, through a comprehensive analysis design, our study seeks to model the effects between three scene visual characteristics, and the factor of temporal variables of session and day, to the RGTs. Our study set [7, 8, 22, 53] works apart, which primarily studied the impact of physical stimuli and biological factors on users' perceived rotation threshold. Our work focuses on the scene visual characteristics and discusses the effect of temporal variables in a controlled overnight experiment, which has never been explored in a similar work [45].

3 EXPERIMENT PROCEDURE

3.1 Preliminary Experiment Settings

Virtual Scenes To answer our research question, the experimental scene design had to encompass dimensions of spatial size, visual density, and realism. A minimum of two-level designs is needed for each dimension. Thus, we first considered the spatial size dimension, following the concept of the AoD [26] and user fixation direction pattern [1] in VR scene design. As [1] found, user fixation direction in environmental scenes focuses more on the horizontal axis, so we designed the landscape scenes with 5 degrees below the user's forward gaze to the scene's horizon line. Conversely, in the room scenes, the floor is positioned about 30 degrees below the user's forward gaze. For the visual density dimension, we followed [44]'s setting where no prominent distractors were placed within the VE in low levels, while visual distractors commonly associated with indoor and outdoor environments, such as furniture and trees, were placed in high levels. Distractors were placed 50 units away from the VR avatar. To exploit the human visual perception of rendered scenes [33] in the realism dimension, two levels of the scene were set differently in terms of texture details, geometry fidelity, and shadows. Notably, we maintained consistent light intensity across all scenes by controlling the main directional light source. With the setting above, we designed a total of $2^3 = 8$ VR scenes in our experiment, and the visual detail of each scene is depicted in Figure 1.

Apparatus We utilized an Oculus Quest 2 headset with controllers as our primary experimental equipment. To develop eight VR scenes, we employed Unreal Engine 5.1 64-bit, integrated with

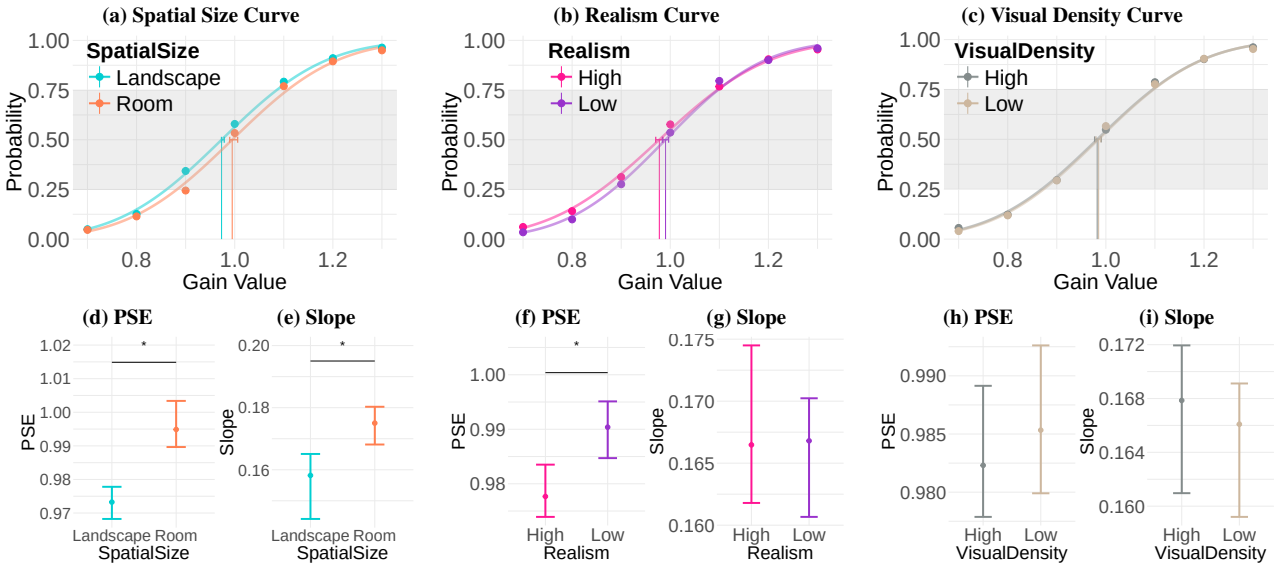

Figure 3: The effects of scene visual characteristics on the psychometric curve and rotation gain thresholds. * indicate significant differences (p<0.05).

the Unreal OpenXR Interface. The Head Mounted Display (HMD) comes equipped with a default 6 Degrees of Freedom (DOF) position and orientation-tracking system that Unreal Engine fully supports. It was connected to a desktop computer via a lengthy cable that did not impede participants' movement, see Figure 2 (first step). All VR scene content was displayed through Meta Quest Link at 60 fps or higher. Both the left-hand and right-hand controllers were utilized for experimental interactions. Participants used the 'X', and 'Y' buttons to respond to questions. Additionally, a real-time head-up interface was designed to aid participants in decision-making, as depicted in Figure 2 (third step).

Pilot Studies We first conduct a pilot study to determine the reasonable measurement range of rotation gain values for the formal user experiments. The range of reasonable gain values for measurement should not be too narrow, as it would hinder the accurate determination of the correct rotation gain thresholds. On the other hand, the range should not be too wide, as it can lead to participant discomfort and increase unnecessary measurements. Five participants aged 19 to 29 were recruited from the university for pilot studies. Eleven levels of rotation gains ranging from 0.5 to 1.5 with increments of 0.1 were randomly arranged in one block and tested on each participant. Participants were required to experience a total of 528 trials (8 scenes × 6 block repetitions × 11 levels of gain) and fill out the Fast Motion Sickness (FMS) questionnaire [25] at the end of each block. The details of each trial will be discussed later.

3.2 Experiment Details

Settings based on Pilot Results The FMS results showed that 4 out of 5 participants exhibited severe motion sickness after completing the second scene. Only 2 out of 5 participants completed the experiments successfully. All participants verbally reported that an extreme gain value caused severe vertigo feeling and the FMS indicated that participants suffer from severe motion sickness after 30 minutes. Consequently, all the extreme values of 0.5, 0.6, 1.4, and 1.5 were removed from the experiment, and 8 experimental scenes were rearranged over 4 consecutive days. On each day, participants were required to complete two VR scenes which took about 30 minutes, including explanations, trials, breaks, and questionnaires, following the empirical settings from previous rotation gain measurement works [10, 60]. In the second round of the pilot study, new settings with a total of 42 trials (7 levels of gains × 6 block repetitions) were tested on each scene. In this round, all 5 newly recruited participants completed the entire experimental procedure with no severe motion sickness observed in FMS results. We then carried out a power analysis for a one-tailed paired-samples t-test on scenes and averaged them to determine the minimum sample size required to achieve a statistical power of at least 0.80. With an alpha level of 0.05 and a medium effect size (Cohen's d = 0.5), the analysis indicated that a sample size of 21 participants is needed. We finalized the setting of our formal study by employing a within-subject study on four consecutive days. The time difference between the two-day experiments had to be overnight and the shortest interval of them was set to 12 hours while the longest interval did not exceed 24 hours from the previous one. Each participant has to go through (4 days x 2 sessions x 6 blocks × 7 gains) of trials to study the effect of (2 spatial size x 2 realism x 2 visual density) scenes' visual characteristics on their perception of rotation gain. The orders of the scenes were assigned according to the Latin Square [15] design. We implemented this study design to balance out the adaptation effects [45] on the perception of rotation gain across eight experimental scenes. This is evident in our extensive analysis, which shows that users' adaptation effects can occur after an overnight break. (see Section 5).

Independent Variable In this study, the independent variables encompass three aforementioned scene visual characteristics, each with two levels of categorical variable mentioned in section 3.1. To verify the effectiveness of our balancing design, we also studied the temporal variable effects of *Session*, and *Day* on the perception

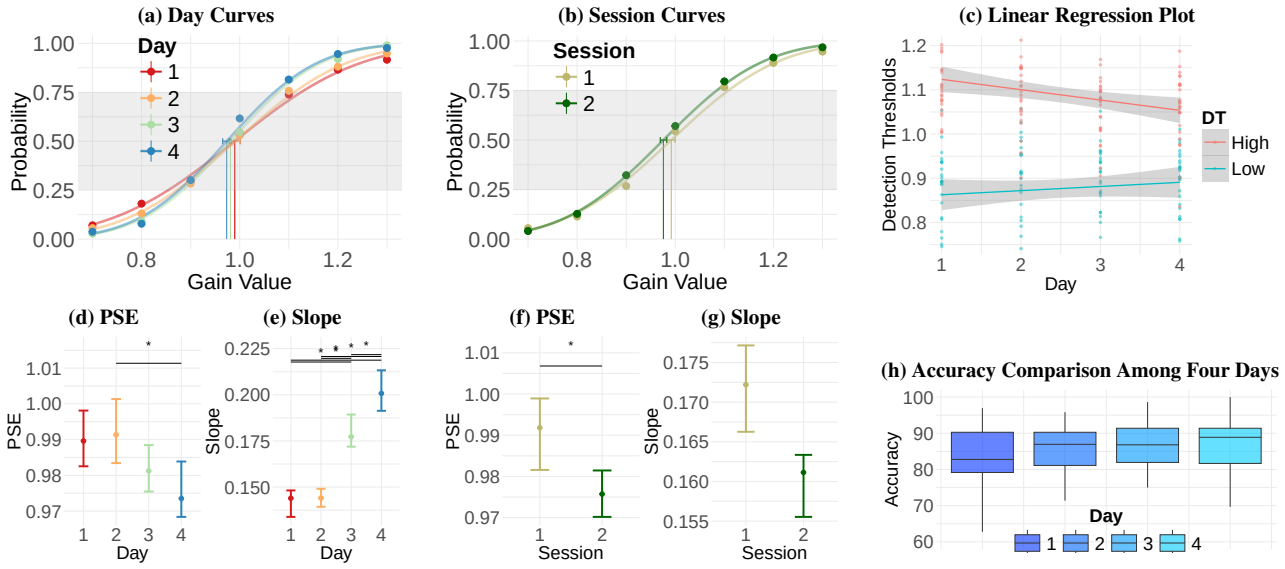

Figure 4: The effects of day and session on psychometric curve and rotation gain thresholds. * indicate significant differences (p< 0.05).

of rotation gain. This will further complement our experiment findings and increase the reproducibility of our results. We separately model scene visual characteristics and temporal variables to avoid multicollinearity and over-fitting. To analyze the scene visual characteristics with LMMs, a linear model was fitted using the *SpatialSize*, *Realism*, and *Visual Density* as fixed effects and *Day*, *Session*, and *Block* as random effects. Conversely, for temporal variables, the fixed and random effects were reversed.

Dependent Variable For dependent variables, we mainly record the user responses to the 2AFC questions, the user accuracy of 2AFC questions in each block, and the user's completion time of each trial. These metrics are later discussed in Section 4 as they are significant in justifying our experiment findings. A Shapiro-Wilk test confirmed that all the collected data are normally distributed.

Task Design of Each Trial The task design of each trial is summarized in Figure 2. A participant was first assigned a random rotation gain ranging from 0.7 to 1.3 when the trial was started. They were required to rotate in place before a head-up user interface was displayed for them to answer the 2AFC question. As sound effects were found to have no impact on gain measurement [42], we employed an audio indicator when the user's rotation angle reached a predetermined limit. It was set at 65° to the left and right of the user's starting position, slightly exceeding the comfortable angle suggested in a previous work [60]. In total, users were limited to rotating four times with magnitude of +65° (right), -130° (left), +130° (right), and -65° (left). Throughout the rotation, the maximum rotation speed limit was set at 45°/s. An alarm sound is triggered when the user rotates too quickly to prevent bias in the results due to rotation speed. The head-up interface will pop out when the rotating task has been completed, participants could use the controller to answer whether they felt their yaw axis rotational speed in the VE was "Faster" or "Slower" compared to the real environment. At the end of each trial, the entire VR screen blackouts for one second to suppress the user's visual-cognition load [29]. Participants were free to remove their HMD immediately if they felt dizzy, experienced motion sickness, or had any other negative reactions.

3.3 Participants

Our study was approved by the board of ethics at Tsinghua University. The recruitment process was disseminated through school email. During the participant recruitment process, we clearly outlined the risks of motion sickness and other potential adverse reactions that may occur during the experiment. To minimize the VR experience learning effect on our study, we purposely indicated that participants should not been exposed to any kind of HMD usage 15 days before starting the formal study. All participants agreed with the terms by signing the consent before joining our formal study. We recruited 29 participants (13 females), aged 19 to 31 (M = 23, SD = 2.34). We focused on individual differences rather than the gender factors in our study. All participants were students or staff members of the university with diverse backgrounds. They all had normal or corrected-to-normal vision and the average interpupillary distance (IPD) was 60.24 cm. All of the participants successfully completed the study.

3.4 Formal Study

In our formal study, participants were first required to complete a Kennedy-Lane Simulator Sickness Questionnaire (SSQ) [24] at the beginning of each experiment scene. We then explained the experimental procedure and objectives to them. The entire experiment commenced after we assisted the user in calibrating their interpupillary distance (IPD) and donning the HMD. The height of the virtual camera was calibrated based on the height of the participant in the physical world. After entering the VR scene, participants first completed five practice trials (with gains of 1.0, 0.7, 1.0, 1.3, and 1.0) to familiarize themselves with the stimulus; correct answers were

provided to the participants for reference after these trials. Following the practice trials, they took part in the formal experiments following the aforementioned trial task design until all 6 blocks of the trial were completed. After finished, each user was given a 10-minute break. Users were directed to another room, where they could report any post-VR simulator symptoms by completing the SSQ during their break. Following the 10-minute break, they were instructed to continue with a second VR scene and followed the same procedure as before. At the end of each day, participants received compensation of $5 for the half-hour experiment.

4 RESULTS

4.1 Psychometric Curve

For each participant's response, we first computed the probability of choosing 'greater' in the 2AFC question, denoted as "Probability" in all the experimental curves following standard procedure from previous works [10, 45, 60, 65]. This can be done by directly find the maximum likelihood of our experimental data using the cumulative normal distribution function with a sigmoidal-shape. The rotation gain thresholds were estimated through the quickpsy version 0.1.5.1. All 95% CI (confidence intervals) of parameters were found using a non-parametric bootstrap procedure with 100 steps. We excluded 39 out of 232 fitted curves that were evenly distributed across 8 scenes, with a dropout rate of 10.75% in all of our studies, due to the bad fitness of curves with high deviance value ($deviance > 10$). The fitted psychometric curves of scene visual characteristics pooled by partipicpants are shown in Figures 3a, 3b,3c, while the pooled curves of temporal variable effect are shown in Figures 4a, 4b.

In our study, fitting a psychometric function estimates four parameters, (i) the PSE, (ii) the LDT, (iii) the HDT, and (iv) the slope. The PSE is the point at which a participant perceives two stimuli as being equal, resulting in a 50% probability of correct gain manipulation detection. Inspired by previous work [45] we also provide a discussion of the fitted curve slope as it indicates the sensitivity of different studying effects on rotation gains. Fitting the function also generates the study effects of PSEs and Slopes. Meanwhile, the LDT and the HDT indicate a 25% and 75% probability of participants detecting the presence of a rotation gain respectively, and they are widely implemented in RDW algorithms. The regions covered by LDT and HDT are shown with a grey background in Figures 3a, 3b,3c, 4a, 4b.

4.2 Linear Mixture Model

To analyze the significance of our study's effects, we used a method of fitting LMMs with both fixed and random effects [35]. Fixed effects account for the influence of the manipulated (independent) variables on the measured outcomes, while random effects account for the unexplained variability due to individual differences (dubbed as UserID) among participants. LMMs independently model each participant's response to the data. Random effects can be modeled as random intercepts, allowing each participant's model intercept to vary based on the best fit to their data. The model fitting was done with the lme4 1.1-35.3 package [3] and the best-fit model was chosen with the buildmer 2.11 [48] package. Before fitting the LMMs, we convert all the categorical variables into binary numerical variables. These Independent numerical variables were then grand-mean centered and all individual data points with z-score exceeded ±3 were excluded as outliers following the steps from [45].

Table 1: Estimated PSE and DTs of eight experiment scenes

VE Configuration	25% LDT	50% PSE	75% HDT
Room x Low Vis x Low Real	0.89	1.00	1.11
Room x Low Vis x High Real	0.88	0.99	1.11
Room x High Vis x Low Real	0.89	1.00	1.10
Room x High Vis x High Real	0.87	0.99	1.11
Landscape x Low Vis x Low Real	0.88	0.98	1.09
Landscape x Low Vis x High Real	0.84	0.96	1.09
Landscape x High Vis x Low Real	0.87	0.98	1.09
Landscape x High Vis x High Real	0.85	0.96	1.08

Table 2: Estimated PSE and DTs of Day and Session

Temporal Configuration	25% LDT	50% PSE	75% HDT
Day 1	0.85	0.99	1.13
Day 2	0.87	0.99	1.11
Day 3	0.88	0.98	1.08
Day 4	0.88	0.97	1.07
Session 1	0.88	0.99	1.11
Session 2	0.87	0.98	1.08

By fitting a LMM, we generate six parameters: (i) the intercept, (ii) the Beta (β), (iii) the standard error of Beta (Std. Error), (iv) t-value, (v) p-value, and (vi) marginal r^2. The intercept indicated the baseline level of the dependent variables when all independent variables (predictors) were zero. Beta explains the effect size of each predictor variable on the dependent variable while the standard error of beta explains the variance of it. t-value explains the ratio of the estimated beta coefficient to its standard error, where the larger t-value provides strong evidence against the null hypothesis. In our study, the p-value demonstrates the level of significance of the independent variables using the "Satterthwaite" method. Marginal r^2 ($m.r^2$) was provided to explain the explanatory power of the fitted model attributable to the fixed predictors. Statistics for the best-fitting models are summarized in Table A and B (see Sections 4.3 and 4.4 for details).

4.3 Effect of Scene Visual Characteristics

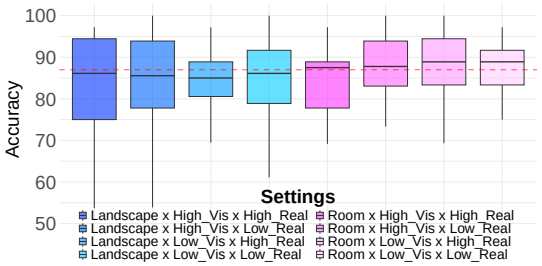

Figure 5: Boxplot of 2AFC questions accuracy of eight experiment scenes. The 87% accuracy is depicted with a red dotted line.

Significant effects were found in the PSEs of *Spatial Size* and *Realism* and no significant difference was found in *Visual Density* (see Figures, 3d, 3f, 3h). In contrast to the PSE, only a significant effect of slope in *Spatial Size* was observed but absent in *Realism* and *Visual Density* (see Figure 3e, 3i,3g). The estimated PSE values and slope values, with their corresponding 95%CI, are summarised in Table D. The pairwise-significant difference demonstrates the PSE in the VR scene with the room settings is higher compared to the landscape settings. Similarly, the slope of the detection curve is steeper in room scenes, indicating that participants have a higher sensitivity to the manipulation compared to landscape scenes. This suggests that *Spatial Size* had a meaningful effect on detecting rotation gain. Although the PSE of *Realism* is significantly different, an effect of the slope values between low and high realism scenes is absent, indicating participants had similar sensitivities in both realism settings. Overall, the mean rotation PSE and the rotation detection thresholds of participants' curves in eight experiment scenes are summarized in Table 1.

To further study the effect of scene visual characteristics on RGTs, the LDT and HDT values of each participant were further analyzed with LMMs. Of the data points, 4.70% were removed as outliers. Both best-fit models of LDT and HDT include *Spatial Size*, *Visual Density*, *Realism*, and all their interactions as fixed effects. For LDT, random effects include Day and UserID. For HDT random effects include UserID, Day, and Block. In both LMM analyses of LDT and HDT, no significant differences or interaction effects were found for the scene's visual characteristics. The fixed effects showed low beta values and standard errors. The low t-values suggest minimal evidence against the null hypothesis, and the p-values indicated no significant differences among the studied effects.

To analyze the dependent variable of trial completion time in different scenes' visual characteristics, we include the factor of rotation gains (0.7 to 1.3) to study whether the intensity of rotation gain applied, will influence the overall task completion and response time of participants in one trail. The best-fit model includes all three scene visual characteristics and their interactions as fixed effects, with the random effects of Visual Density, Day, and Block. No significant effect nor interaction effect was observed. The best explanation would be that participants experienced and completed one trial persistently throughout the experiments, regardless of three studied visual characteristics and the intensity of rotation gains, this observation is similar to the previous work [45]. To study the effect of different scenes' visual characteristics on 2AFC question accuracy within each block of trials, we first dropped the gain value of 1.0 in our collected user data. Then, we count the percentage of user accuracy in the 6 remaining gains trials by comparing user response to the ground truth. After removing 5.75% of outlier data, a linear model was fitted on the remaining data. The best-fit model of accuracy includes all three scene visual characteristics and their interactions as fixed effects with the random effects of UserID, Day, and Block. A significant effect ($t(1376) = 2.013, p = 0.046, m.r^2 = 0.022$) was found in the analysis factor of *Spatial Size*. When we compared the accuracy across 8 studied scenes with a boxplot in Figure 5, participants appeared to have slightly higher accuracy in room settings, which aligns with the higher slope value observed in Figure 3e, suggesting a potential increase in sensitivity to rotation gains in room settings.

4.4 Effect of Temporal Variables

To study the influence of short-interval, temporal variable effects on the rotation gains, the factors of *Day* and *Session* are included. Due to the Latin square design, the PSEs saw no significant effect across all four experiment days. The only exception was between Day 2 and Day 4 as a decreasing trend of PSE was observed (see Figure 4d). Similarly, a significant effect of PSE was found between sessions 1 and 2 (see Figure 4f). A significant effect of *Day* on the slope was consistently observed (see Figure 4e). The slope showed a consistent increasing trend over multiple days. It began at a value of 0.15 and rose steadily, reaching 0.20 by the final day. When comparing the slope values between consecutive days, statistically significant differences were detected for nearly all day-to-day comparisons. The only exception was between day 1 and day 2, where the slope did not exhibit a notable change during that specific period. Apart from that, the slope demonstrated an ascending pattern across the days (see Figure 4e and 4a). This suggests that *Day* had a meaningful effect on the slope of the detection curve. However, the *Session* slope shows no significant effect, indicating that, the user's sensitivity of rotation gain is not different from two sessions within a day. This indicated that it had no meaningful effect and this result agreed with all the empirical works [10, 60] where a carry-over effect did not occur in two consecutive experiment sessions, even when a participant was exposed to VR scenes with different visual characteristics settings in our study. The estimated PSE and detection threshold values are summarized in Table E and 2. Overall, *Session* has almost negligible impact on the PSE values in our study.

To further study the effect of *Day* and *Session*, the LDT and HDT values of each participant were then analyzed using LMMs method. Of the data points, 4.72% were removed as outliers. Both best-fit models of LDT and HDT include *Day*, *Session*, and their interaction as fixed effects. Both LDT and HDT have the same random effects in UserID and SpatialSize. A significant difference ($t(1089) = 3.235, p = 0.001, m.r^2 = 0.0098$) was found in the *Day* effect for LDT. Meanwhile, no significant effect was found in *Session* nor interaction effect was found between *Day* and *Session*. For HDT, apart from the *Day* effect ($t(1089) = -3.350, p < 0.001, m.r^2 = 0.049$), no significant effect was found in *Session* nor interaction effect was found between *Day* and *Session* for HDT. In Table B, LDT and HDT section, a low beta, and standard error were observed for *Day*, but the high t-value indicates that the model has high evidence of rejecting the null hypothesis while demonstrating extremely low p-values $p < 0.001$ in both LDT and HDT. To delve in further, we plot out both the box plot and the linear regression of data and observed an apparent trend in both LDT and HDT. Both values converge to the gain value of 1 across days as depicted in Figure 4c. To study the temporal variable effects on the trial completion time, we used the same data processing steps mentioned in section 4.3 but we included the block as an additional fixed effect this time. A 6.01% of outlier data was removed and the best-fit model of trial completion time includes *Day*, *Session*, *Block*, *Gain* and all their interactions as fixed effects, with the random effects of UserID and Block. No significant effect nor interaction effect was observed, which indicated that throughout the experiments, participants experienced and completed one trial in similar time lengths, regardless of any temporal effect and the intensity of rotation gains. Similarly, in the

accuracy analysis using LMMs, we used the same data processing steps mentioned in section 4.3 for computing accuracy. After removing 5.75% of outlier data, the best-fit model of accuracy includes *Day*, *Session*, *Block*, and all their interactions as fixed effects, with the random effects of UserID and SpatialSize. A significant effect ($t(1376) = 3.846, p < 0.001, m.r^2 = 0.011$) was found with the setting of *Day*. When we compared the accuracy across 4 studied days with a boxplot in Figure 4h, it is obvious that participants have a rising trend of accuracy across the days. The trend is coherent with the findings of increasing slope value in 4e from Day 1 to Day 3, which also explains why the RGTs of participants converge across the days, as depicted in Figure 4c.

Table 3: LMMs Parameters of SSQ Delta scores

Fixed Effect	β	Std. Error	t (236)	$p-value$	$m.r^2$
Nausea					
(Intercept)	3.984	2.102	1.896	0.059	1.8e-02
Day	0.325	1.107	0.293	0.769	4.1e-04
Session	−4.267	2.853	−1.495	0.136	1.1e-02
Day:Session	−0.013	1.560	−0.008	0.994	3.2e-07
Disorientation					
(Intercept)	14.807	4.386	3.376	0.001	6.9e-02
Day	−1.361	2.150	−0.633	0.528	1.9e-03
Session	−6.419	5.528	−1.161	0.247	6.6e-03
Day:Session	−0.781	3.021	−0.258	0.796	3.3e-04
Oculomotor					
(Intercept)	3.965	1.707	2.323	0.021	2.7e-02
Day	0.506	0.898	0.563	0.574	1.5e-03
Session	−4.473	2.314	−1.933	0.055	1.8e-02
Day:Session	−0.194	1.264	−0.153	0.878	1.2e-04
Overall					
(Intercept)	4.927	1.472	3.346	0.001	6.3e-02
Day	−0.269	0.739	−0.364	0.716	6.4e-04
Session	−2.762	1.900	−1.454	0.148	1.0e-02
Day:Session	−0.237	1.038	−0.228	0.820	2.5e-04

4.5 Simulator Sickness

We measured simulator sickness by analyzing the SSQ submitted by the user, and followed the standard procedure listed in [24] to calculate the SSQ total score. We first fitted LMMs to study the three VR scene visual characteristics following the same procedure in 4.3 to study their influence to the SSQ total score. However, we observed no significant difference or interference in them. This indicated that participants experienced an equal amount of sickness regardless of VR scene visual characteristics throughout the four-day experiment. We then applied the same methods to study the SSQ total score over the temporal variables. For *session*, we found a pairwise significant difference between Session 1 Start- Session 1 End, Session 1 Start-Session 2 End, and Session 2 Start - Session 2 End as depicted in Figure 6, while the SSQ total scores are generally lower compared to previous work [45]. No pairwise significant effects were observed for *Day*.

To further study the users' difference in SSQ score in each session of four days, we followed the previous method [10] to compute the delta of SSQ score, (i.e. end of session score minus start of session score) and fit LMMs with each of the four SSQ factors. In Table 3, we observed no significant difference in four delta SSQ factors over the *Session* and *Day*, indicating that the users' state was equivalent at the end of both VR scenes, and user perception of rotation gains is equal in both sessions. This result is consistent with the previous experiments [10, 18, 53, 60].

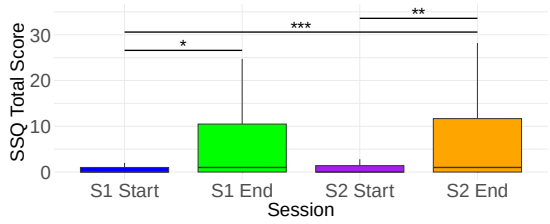

Figure 6: The SSQ total score recorded in the session 1 start, session 2 end, session 2 start, and session 2 end. * denotes $0.01 < p < 0.05$; ** denoted $0.001 < p < 0.01$; * denotes $p < 0.001$.**

5 DISCUSSION

Our main objective is to assess whether different VR scenes with varying visual characteristics or temporal variables alter the perception of rotation gains in VEs. In this section, we integrated all the independent variables studied in our experiment for an in-depth discussion.

Findings Through the results of psychometric curve analysis, we conclude that only the scene visual characteristics of *Spatial Size* significantly influence the perception of rotational speed, as both fitted parameters of PSE and slope were significantly different. While the sensitivity of the participants in room settings is significantly higher, the accuracy of participants' trials is also generally higher in room settings through the LMM parameters analysis. We did not observe a significant difference in RGTs among the three scene visual characteristics through LMM analysis. However, we observed both the RGTs are higher in room settings as compared to landscape settings, as evident in Table 1. The trial completion time was not significantly different among the three scene visual characteristics and gain, indicating that the user completed the rotation task and answered 2AFC questions in a similar time interval. It is worth noting that, all the fixed effect's intercepts are strongly significantly different ($p < 0.001$) from zero, and the baseline (intercept) results are highly unlikely to have occurred by random chance.

Our measured RGTs in Table 1 generally fall within the range of previously recorded rotation gain thresholds, spanning from 0.84 to 1.41. Despite the exclusion of gains 0.5, 0.6, 1.4, and 1.5 in our experiment, and our measured values being skewed more towards 1, our results still closely align with the measurements reported in Paludan *et al.*'s work [44]. Importantly, other studies on rotation gain introduce visual navigation indicators such as arrows or pointers [10, 60, 67] to guide the user, potentially influencing their perception of rotation speed. Our work eliminates such additional factors.

With the balancing effect, we did not observe any interactions among the three scene visual characteristics through LMMs analysis. These results reassure the findings from previous work [44] in most

cases in which users are insensitive to the visual density when the virtual scene is complex. One possible explanation is that the foveated attention is not fixed on certain objects when users are rotating, unlike translation [43]. In the dimension of realism, our study aligned with a previous study on translation gain[59] that different textures and global illumination do not affect perception. For *spatial size*, one possible explanation of the significant effect might be that the AoD is an important cue to egocentric distance perception in VE [14] and PSE value can be influenced by the AoD, as shown in Figure 3a. However, this finding requires further verification, as the effect size of accuracy, indicated by a small marginal r^2 of 0.022, suggests that the model explains only a limited portion of the variance, as depicted in the spatial size accuracy section in Table A.

Another interesting finding from our experiment is that, even though a Latin Square design was implemented, we still observed an adaptation effect in our experiment. In Table B, we see *Day* has a significant effect on LDT, HDT, and Accuracy, but is not significant for Trail Completion Time. The range of detection thresholds skewed inwards towards the PSE value across four overnight sessions and increasing sensitivity from day 1 to 4, see Table 2, and evidenced by the result of the temporal effects psychometric curve in Figure 4a. This pattern extends the findings from previous works [45], indicating an adaptation effect in VR users can occur over *Day*, with an overnight break, compared to weeks. Furthermore, these counterbalanced effects observed throughout the four days may also explain why we achieved tighter rotation gain thresholds. Based on our rigorous analysis on the temporal variables, the resulting adaptation effects have a higher impact on the perception of rotation speed and RGTs, as compared to the scene visual characteristic, based on the p-value results obtained in Table A and B.

Surprisingly, our findings differ from those of Bölling *et al.*[4], who found that increased exposure to curvature gain decreased sensitivity to manipulation. Our study shows that increased exposure increased sensitivity. This difference might arise from variations in experimental conditions or the specific types of gain manipulations used. The divergent result of RGTs in Figure 4c highlights the need for further research to understand how different factors, such as the type and duration of exposure, influence sensitivity to manipulation.

Application In terms of rotation gain application, our results suggest adjusting rotation gain thresholds based on the spatial size of the VR scene. For instance, one may apply lower RGT values in landscape settings, as depicted in Table 1. We recommend VR application developers adjust the PSE value and DTs, based on the results in Table 1. In a landscape scene, the PSE value and DTs are recommended to be set 0.1 lower than the room settings. Our findings can potentially support user-centered gain recommendation methods and dynamic gain adjustment methods based on the *Spatial Size* of VE. In the future, our discoveries can be integrated into a VR content analysis system to extract the semantics of VR scenes and intelligently adjust the LDT, HDT, and PSE. Our work's findings can also serve as the guidelines for VR content generation.

The second application of our work suggests that we consider manipulating the detection thresholds for rotation gains based on the VR longitudinal usage of the user [45]. We found that our participants have "learned" the rotation gains across time, in our four-day experiment. This indicated that such learning ability might be related to the ability to adapt to the gain during VR navigation. Together with previous work, the insights generated by our work suggested that gain can be something to "learn" and it can adjusted dynamically in redirection controllers based on users' time usage patterns.

6 LIMITATION AND FUTURE WORK

The first limitation of our work is the lack of experimental power by using the two-level categorical variables in three scene visual characteristics, rather than using continuous variables. For now, the three primary factors in this study are predominantly defined in semantic terms rather than through highly precise, quantification of what constitutes low visual density and low realism in a VR scene. Further studies on various levels of realism and visual density that can be quantitatively defined are needed. Based on our findings, an experiment setting with continuous AoD in VE design is worth exploring for modeling the rotation gain DTs given different spatial sizes in different VEs. Our current results only demonstrate an effect on PSEs and slope values, with a small effect size for accuracy, and neither RGT in this dimension showed a significant effect. These limitations might be due to the medium sample size used in our 2x2x2 experimental design. In addition, investigating the correlation between the time interval and the level of rotation gain adaptation will be an interesting topic to explore. For example, whether the rotation gain adaptation effect will be more pronounced when a user is constantly exposed to rotation gain in a shorter time interval (day) as compared to a longer time interval (week)? By considering the effects of scene visual characteristics and time usage patterns (i.e., learning mechanisms) together, the applicability of threshold ranges can be optimized for user personalization, thus benefiting applications such as real-time VR content generation.

Secondly, we excluded the extreme values (0.5, 0.6, 1.4, and 1.5) of rotation gain that were commonly examined in previous studies and did not test them in this experiment. This had a direct impact on the fitted range of rotation gain thresholds, causing the RGTs values to be closer to 1 compared to previous works. In the future, adding the response of the user towards extreme values is expected to bring the fitted values closer to the previous work. Furthermore, the effects of dynamic objects such as avatars or interactive objects on rotation gain thresholds should also be further investigated.

7 CONCLUSION

In this study, we examined the effects of scene visual characteristics and short-term temporal variables on the perception of rotation speed in a fully immersed VR environment. By explicitly designing eight experimental conditions, we found significant differences in the PSE where participants are more sensitive in the room settings compared with the landscape settings. The significant effects of participants' sensitivity to visual density and realism are not found. Additionally, in a temporal analysis, we found that our participants have "learned" to detect the rotation gains, in a four-day experiment. Both PSE and RGTs have shown significant effects as participants' sensitivity and accuracy are increasing over days. A lower p-value in LLM analysis indicated that the short-term temporal effect of overnight break is another predominant factor, even when users experience different visual stimuli in VEs, such as different visual characteristic settings in our study.

ACKNOWLEDGMENTS

This work was supported by the National Key Research and Development Program of China (No. 2023YFF0905104), the National Natural Science Foundation of China (No. 62361146854), Tsinghua-Tencent Joint Laboratory for Internet Innovation Technology, and the Marsden Fund Council managed by the Royal Society of New Zealand under Grant MFP-20-VUW-180.

REFERENCES

[1] Avi M. Aizenman, George A. Koulieris, Agostino Gibaldi, Vibhor Sehgal, Dennis M. Levi, and Martin S. Banks. 2023. The Statistics of Eye Movements and Binocular Disparities during VR Gaming: Implications for Headset Design. *ACM Trans. Graph.* 42, 1, Article 7 (jan 2023), 15 pages. https://doi.org/10.1145/3549529

[2] Eric R. Bachmann, Eric Hodgson, Cole Hoffbauer, and Justin Messinger. 2019. Multi-User Redirected Walking and Resetting Using Artificial Potential Fields. *IEEE Transactions on Visualization and Computer Graphics* 25, 5 (2019), 2022–2031. https://doi.org/10.1109/TVCG.2019.2898764

[3] Douglas Bates, Martin Mächler, Ben Bolker, and Steve Walker. 2023. *lme4: Linear Mixed-Effects Models using 'Eigen' and S4*. https://CRAN.R-project.org/package=lme4 R package version 1.1-32.

[4] Luke Bölling, Niklas Stein, Frank Steinicke, and Markus Lappe. 2019. Shrinking circles: Adaptation to increased curvature gain in redirected walking. *IEEE transactions on visualization and computer graphics* 25, 5 (2019), 2032–2039.

[5] Doug Bowman, Ernst Kruijff, Joseph J LaViola Jr, and Ivan P Poupyrev. 2004. *3D User interfaces: theory and practice, CourseSmart eTextbook*. Addison-Wesley.

[6] Matthew H. E. M. Browning, Katherine J. Mimnaugh, Carena J. van Riper, Heidemarie K. Laurent, and Steven M. LaValle. 2020. Can Simulated Nature Support Mental Health? Comparing Short, Single-Doses of 360-Degree Nature Videos in Virtual Reality With the Outdoors. *Frontiers in Psychology* 10 (2020). https://doi.org/10.3389/fpsyg.2019.02667

[7] Gerd Bruder, Victoria Interrante, Lane Phillips, and Frank Steinicke. 2012. Redirecting Walking and Driving for Natural Navigation in Immersive Virtual Environments. *IEEE Transactions on Visualization and Computer Graphics* 18, 4 (2012), 538–545. https://doi.org/10.1109/TVCG.2012.55

[8] Gerd Bruder, Frank Steinicke, Klaus H. Hinrichs, and Harald Frenz. [n. d.]. Impact of Gender on Discrimination between Real and Virtual Stimuli.

[9] Gerd Bruder, Frank Steinicke, Phil Wieland, and Markus Lappe. 2011. Tuning self-motion perception in virtual reality with visual illusions. *IEEE Transactions on Visualization and Computer Graphics* 18, 7 (2011), 1068–1078.

[10] Hugo Brument, Maud Marchal, Maud Marchal, Anne-Hélène Olivier, and Ferran Argelaguet Sanz. 2021. Studying the Influence of Translational and Rotational Motion on the Perception of Rotation Gains in Virtual Environments. *Symposium on Spatial User Interaction* (2021). https://doi.org/10.1145/3485279.3485282

[11] Hugo Brument, Maud Marchal, Anne-Hélène Olivier, and Ferran Argelaguet. 2020. Influence of dynamic field of view restrictions on rotation gain perception in virtual environments. In *Virtual Reality and Augmented Reality: 17th EuroVR International Conference, EuroVR 2020, Valencia, Spain, November 25–27, 2020, Proceedings 17*. Springer, 20–40.

[12] Ben J. Congdon and Anthony Steed. 2019. Sensitivity to Rate of Change in Gains Applied by Redirected Walking. *Virtual Reality Software and Technology* (2019). https://doi.org/10.1145/3359996.3364277

[13] Henry E. Cook, Justin A. Hassebrock, and L. James Smart. 2018. Responding to Other People's Posture: Visually Induced Motion Sickness From Naturally Generated Optic Flow. *Frontiers in Psychology* (2018). https://doi.org/10.3389/fpsyg.2018.01901

[14] Sarah H. Creem-Regehr, Jeanine K. Stefanucci, and Bobby Bodenheimer. 2022. Perceiving distance in virtual reality: theoretical insights from contemporary technologies. *Philosophical Transactions of the Royal Society B: Biological Sciences* 378, 1869 (Dec. 2022). https://doi.org/10.1098/rstb.2021.0456

[15] Y. Dodge. 2008. *The Concise Encyclopedia of Statistics*. Springer New York. https://books.google.com.my/books?id=k2zklGOBRDwC

[16] Walter H. Ehrenstein and Addie Ehrenstein. 1999. *Psychophysical Methods*. Springer Berlin Heidelberg, Berlin, Heidelberg, 1211–1241. https://doi.org/10.1007/978-3-642-58552-4_43

[17] Jacqueline M. Fulvio, Mohan Ji, and Bas Rokers. 2021. Variations in visual sensitivity predict motion sickness in virtual reality. *Entertainment Computing* 38 (2021), 100423. https://doi.org/10.1016/j.entcom.2021.100423

[18] Timofey Grechkin, Jerald Thomas, Mahdi Azmandian, Mark Bolas, and Evan Suma. 2016. Revisiting Detection Thresholds for Redirected Walking: Combining Translation and Curvature Gains. In *Proceedings of the ACM Symposium on Applied Perception* (Anaheim, California) *(SAP '16)*. Association for Computing Machinery, New York, NY, USA, 113–120. https://doi.org/10.1145/2931002.2931018

[19] Cole Hoffbauer. 2018. *Multi-user redirected walking and resetting utilizing artificial potential fields*. Ph. D. Dissertation. http://rave.ohiolink.edu/etdc/view?acc_num=miami1530629793552698

[20] Seokjun Hong, Gerard J. Kim, and Gerard Jounghyun Kim. 2016. Accelerated viewpoint panning with rotational gain in 360 degree videos. *Virtual Reality Software and Technology* (2016). https://doi.org/10.1145/2993369.2996309

[21] Courtney Hutton, Shelby Ziccardi, Julio Medina, and Evan Suma Rosenberg. 2018. Individualized Calibration of Rotation Gain Thresholds for Redirected Walking. In *ICAT-EGVE 2018 - International Conference on Artificial Reality and Telexistence and Eurographics Symposium on Virtual Environments*. The Eurographics Association;, 61–64. https://doi.org/10.2312/egve.20181315

[22] Philip Jaekl, Michael Jenkin, and Laurence R. Harris. 2005. Perceiving a stable world during active rotational and translational head movements. *Experimental Brain Research* (2005). https://doi.org/10.1007/s00221-004-2191-8

[23] Stephen Kaplan. 1995. The restorative benefits of nature: Toward an integrative framework. *Journal of Environmental Psychology* 15, 3 (1995), 169–182. https://doi.org/10.1016/0272-4944(95)90001-2 Green Psychology.

[24] Robert S. Kennedy, Norman E. Lane, Kevin S. Berbaum, and Lilienthal Mg. 1993. Simulator Sickness Questionnaire: An enhanced method for quantifying simulator sickness. *The International Journal of Aviation Psychology* (1993).

[25] Behrang Keshavarz and Heiko Hecht. 2011. Validating an Efficient Method to Quantify Motion Sickness. *Human factors* 53 (08 2011), 415–26. https://doi.org/10.1177/0018720811403736

[26] Dooyoung Kim, Jinwook Kim, Jae eun Shin, Boram Yoon, Jeongmin Lee, and Woontack Woo. 2022. Effects of Virtual Room Size and Objects on Relative Translation Gain Thresholds in Redirected Walking. *IEEE Conference on Virtual Reality and 3D User Interfaces* (2022).

[27] Dooyoung Kim, Jae-eun Shin, Jeongmi Lee, and Woontack Woo. 2021. Adjusting Relative Translation Gains According to Space Size in Redirected Walking for Mixed Reality Mutual Space Generation. In *2021 IEEE Virtual Reality and 3D User Interfaces (VR)*. 653–660. https://doi.org/10.1109/VR50410.2021.00091

[28] Lucie Kruse, Eike Langbehn, and Frank Stelnlcke. 2018. I Can See on My Feet While Walking: Sensitivity to Translation Gains with Visible Feet. *IEEE Conference on Virtual Reality and 3D User Interfaces* (2018). https://doi.org/10.1109/vr.2018.8446216

[29] Eike Langbehn, Frank Steinicke, Markus Lappe, Gregory F Welch, and Gerd Bruder. 2018. In the blink of an eye: leveraging blink-induced suppression for imperceptible position and orientation redirection in virtual reality. *ACM Transactions on Graphics (TOG)* 37, 4 (2018), 1–11.

[30] Dong-Yong Lee, Yong-Hun Cho, and In-Kwon Lee. 2019. Real-time Optimal Planning for Redirected Walking Using Deep Q-Learning. In *2019 IEEE Conference on Virtual Reality and 3D User Interfaces (VR)*. 63–71. https://doi.org/10.1109/VR.2019.8798121

[31] Jieun Lee, Seokhyun Hwang, Aya Ataya, and SeungJun Kim. 2024. Effect of optical flow and user VR familiarity on curvature gain thresholds for redirected walking. *Virtual Reality* 28, 1 (29 Jan 2024), 35.

[32] Tiffany Luong and Christian Holz. 2022. Characterizing Physiological Responses to Fear, Frustration, and Insight in Virtual Reality. *IEEE Transactions on Visualization and Computer Graphics* (2022), 1–11. https://doi.org/10.1109/TVCG.2022.3203113

[33] Ann McNamara. 2001. Visual Perception in Realistic Image Synthesis. *Computer Graphics Forum* (2001). https://doi.org/10.1111/1467-8659.00550

[34] Justin Messinger, Eric Hodgson, and Eric R. Bachmann. 2019. Effects of Tracking Area Shape and Size on Artificial Potential Field Redirected Walking. In *2019 IEEE Conference on Virtual Reality and 3D User Interfaces (VR)*. 72–80. https://doi.org/10.1109/VR.2019.8797818

[35] Lotte Meteyard and Robert A.I. Davies. 2020. Best practice guidance for linear mixed-effects models in psychological science. *Journal of Memory and Language* 112 (2020), 104092. https://doi.org/10.1016/j.jml.2020.104092

[36] Fariba Mostajeran, Marvin Fischer, Frank Steinicke, and Simone Kühn. 2023. Effects of exposure to immersive computer-generated virtual nature and control environments on affect and cognition. *Scientific Reports* 13, 1 (05 Jan 2023), 220. https://doi.org/10.1038/s41598-022-26750-6

[37] Fariba Mostajeran, Jessica Krzikawski, Frank Steinicke, and Simone Kühn. 2021. Effects of exposure to immersive videos and photo slideshows of forest and urban environments. *Scientific Reports* 11, 1 (17 Feb 2021), 3994. https://doi.org/10.1038/s41598-021-83277-y

[38] Fariba Mostajeran, Sebastian Schneider, Gerd Bruder, Simone Kühn, and Frank Steinicke. 2024. Analyzing Cognitive Demands and Detection Thresholds for Redirected Walking in Immersive Forest and Urban Environments. In *2024 IEEE Conference Virtual Reality and 3D User Interfaces (VR)*. 61–71. https://doi.org/10.1109/VR58804.2024.00030

[39] H Nakamura, T Aoki, F Okuyama, and H Tanaka. 1996. Development of virtual reality (VR) system to evaluate human 3D spatial cognition [eye movements analysis]. In *Proceedings of 18th Annual International Conference of the IEEE Engineering in Medicine and Biology Society*, Vol. 2. IEEE, 650–651.

[40] M. Newman, B. Gatersleben, K.J. Wyles, and E. Ratcliffe. 2022. The use of virtual reality in environment experiences and the importance of realism. *Journal of*

Environmental Psychology 79 (2022), 101733. https://doi.org/10.1016/j.jenvp.2021.101733

[41] Niels Christian Nilsson, Tabitha Peck, Gerd Bruder, Eri Hodgson, Stefania Serafin, Mary Whitton, Frank Steinicke, and Evan Suma Rosenberg. 2018. 15 Years of Research on Redirected Walking in Immersive Virtual Environments. *IEEE Computer Graphics and Applications* 38, 2 (2018), 44–56. https://doi.org/10.1109/MCG.2018.111125628

[42] Niels Christian Nilsson, Evan A. Suma, Rolf Nordahl, Mark Bolas, and Stefania Serafin. 2016. Estimation of detection thresholds for audiovisual rotation gains. *null* (2016). https://doi.org/10.1109/vr.2016.7504743

[43] Kazuya Otake, Shogo Okamoto, Yasuhiro Akiyama, and Yoji Yamada. 2022. Magnitude estimation of self-speed under different visual cue conditions in virtual space. In *2022 IEEE 4th Global Conference on Life Sciences and Technologies (LifeTech)*. IEEE, 401–403.

[44] Anders Paludan, Jacob Elbaek, Mathias Mortensen, Morten Zobbe, Niels Christian Nilsson, Rolf Nordahl, Lars Reng, and Stefania Serafin. 2016. Disguising rotational gain for redirected walking in virtual reality: Effect of visual density. In *2016 IEEE Virtual Reality (VR)*. 259–260.

[45] Andrew Robb, Kristopher Kohm, and John Porter. 2022. Experience Matters: Longitudinal Changes in Sensitivity to Rotational Gains in Virtual Reality. *ACM Trans. Appl. Percept.* 19, 4, Article 16 (nov 2022), 18 pages. https://doi.org/10.1145/3560818

[46] Yannick Rothacher, Anh Nguyen, Bigna Lenggenhager, Andreas Kunz, and Peter Brugger. 2018. Visual capture of gait during redirected walking. *Scientific Reports* (2018). https://doi.org/10.1038/s41598-018-36035-6

[47] Shyam Prathish Sargunam, Kasra Rahimi Moghadam, Mohamed Suhail, and Eric D Ragan. 2017. Guided head rotation and amplified head rotation: Evaluating semi-natural travel and viewing techniques in virtual reality. In *2017 IEEE Virtual Reality (VR)*. IEEE, 19–28.

[48] C. Scheepers. 2023. *buildmer: Stepwise Elimination and Term Reordering for Mixed-Effects Regression*. https://CRAN.R-project.org/package=buildmer R package version 1.7.

[49] Razzaque Sharif, Kohn Zachariah, and Whitton Mary, C. 2001. Redirected Walking. In *In Proceedings of Eurographics,ACM*. 289–294.

[50] L. James Smart, Edward W. Otten, Adam J. Strang, Eric M. Littman, and Henry E. Cook. 2014. Influence of Complexity and Coupling of Optic Flow on Visually Induced Motion Sickness. *Ecological Psychology* (2014). https://doi.org/10.1080/10407413.2014.958029

[51] Richard H. Y. So, W. T. Lo, and Andy T. K. Ho. 2001. Effects of Navigation Speed on Motion Sickness Caused by an Immersive Virtual Environment. *Human Factors* 43, 3 (2001), 452–461. https://doi.org/10.1518/001872001775898223 arXiv:https://doi.org/10.1518/001872001775898223 PMID: 11866200.

[52] Patrick J Sparto, Susan L Whitney, Larry F Hodges, Joseph M Furman, and Mark S Redfern. 2004. Simulator sickness when performing gaze shifts within a wide field of view optic flow environment: preliminary evidence for using virtual reality in vestibular rehabilitation. *Journal of NeuroEngineering and Rehabilitation* 1, 1 (Dec. 2004), 14.

[53] Frank Steinicke, Gerd Bruder, Jason Jerald, Harald Frenz, and Markus Lappe. 2010. Estimation of Detection Thresholds for Redirected Walking Techniques. *IEEE Transactions on Visualization and Computer Graphics* 16 (2010).

[54] Qi Sun. 2021. Leveraging human visual perception for an optimized virtual reality experience. *IEEE Computer Graphics and Applications* 41, 6 (2021), 164–170.

[55] Jerald Thomas and Evan Suma Rosenberg. 2019. A General Reactive Algorithm for Redirected Walking Using Artificial Potential Functions. In *2019 IEEE Conference on Virtual Reality and 3D User Interfaces (VR)*. 56–62. https://doi.org/10.1109/VR.2019.8797983

[56] Deltcho Valtchanov, Kevin R. Barton, and Colin Ellard. 2010. Restorative Effects of Virtual Nature Settings. *Cyberpsychology, Behavior, and Social Networking* 13, 5 (2010), 503–512. https://doi.org/10.1089/cyber.2009.0308 arXiv:https://doi.org/10.1089/cyber.2009.0308 PMID: 20950174.

[57] Koorosh Vaziri, Peng Liu, Sahar Aseeri, and Victoria Interrante. 2017. Impact of visual and experiential realism on distance perception in VR using a custom video see-through system. In *Proceedings of the ACM Symposium on Applied Perception*. 1–8.

[58] Roshan Venkatakrishnan, Rohith Venkatakrishnan, Balagopal Raveendranath, Christopher C. Pagano, Andrew C. Robb, Wen-Chieh Lin, and Sabarish V. Babu. 2023. How Virtual Hand Representations Affect the Perceptions of Dynamic Affordances in Virtual Reality. *IEEE Transactions on Visualization and Computer Graphics* 29, 5 (2023), 2258–2268. https://doi.org/10.1109/TVCG.2023.3247041

[59] Kristoffer Waldow, Arnulph Fuhrmann, and Stefan M. Grünvogel. 2018. Do Textures and Global Illumination Influence the Perception of Redirected Walking Based on Translational Gain?. In *2018 IEEE Conference on Virtual Reality and 3D User Interfaces (VR)*. 717–718. https://doi.org/10.1109/VR.2018.8446587

[60] Chen Wang, Song-Hai Zhang, Yizhuo Zhang, Stefanie Zollmann, and Shi-Min Hu. 2022. On Rotation Gains Within and Beyond Perceptual Limitations for Seated VR. https://doi.org/10.48550/ARXIV.2203.02750

[61] William H. Warren, Bruce A. Kay, Wendy D. Zosh, Andrew P. Duchon, and Stephanie Sahuc. 2001. Optic flow is used to control human walking. *Nature Neuroscience* 4, 2 (01 Feb 2001), 213–216.

[62] Felix A. Wichmann and N. Jeremy Hill. 2001. The psychometric function: I. Fitting, sampling, and goodness of fit. *Perception & Psychophysics* 63, 8 (01 Nov 2001), 1293–1313. https://doi.org/10.3758/BF03194544

[63] Betsy Williams, Gayathri Narasimham, Bjoern Rump, Timothy P. McNamara, Thomas H. Carr, John Rieser, and Bobby Bodenheimer. 2007. Exploring Large Virtual Environments with an HMD When Physical Space is Limited. In *Proceedings of the 4th Symposium on Applied Perception in Graphics and Visualization* (Tubingen, Germany) *(APGV '07)*. Association for Computing Machinery, New York, NY, USA, 41–48. https://doi.org/10.1145/1272582.1272590

[64] Niall L. Williams, Aniket Bera, and Dinesh Manocha. 2021. ARC: Alignment-based Redirection Controller for Redirected Walking in Complex Environments. *CoRR* abs/2101.04912 (2021). arXiv:2101.04912 https://arxiv.org/abs/2101.04912

[65] Niall L. Williams and Tabitha C. Peck. 2019. Estimation of Rotation Gain Thresholds Considering FOV, Gender, and Distractors. *IEEE Transactions on Visualization and Computer Graphics* (2019).

[66] Sen-Zhe Xu, Tian Lv, Guangrong He, Chia-Hao Chen, Fang-Lue Zhang, and Song-Hai Zhang. 2022. Optimal Pose Guided Redirected Walking with Pose Score Precomputation. In *2022 IEEE Conference on Virtual Reality and 3D User Interfaces (VR)*. 655–663. https://doi.org/10.1109/VR51125.2022.00086

[67] Jingxin Zhang, Eike Langbehn, Dennis Krupke, Nicholas Katzakis, and Frank Steinicke. 2018. Detection Thresholds for Rotation and Translation Gains in 360° Video-Based Telepresence Systems. *IEEE Transactions on Visualization and Computer Graphics* 24, 4 (2018), 1671–1680. https://doi.org/10.1109/TVCG.2018.2793679

A APPENDIX TABLE 1

Table 4: Scene Visual Characteristic effects of Spatial Size, Realism, and Visual Density Models Parameters. Bold values denote the statistical significance of p < 0.05.

Fixed Effect	β	Std. Error	t (n)	$p-value$	$m.r^2$
LDT			(n = 1089)		
(Intercept)	0.918	0.017	54.558	**<0.001**	9.8e-01
Realism	0.022	0.014	1.534	0.125	2.3e-03
VisualDensity	0.002	0.014	0.122	0.903	1.4e-05
SpatialSize	0.024	0.018	1.383	0.170	2.1e-02
Realism:VD	0.002	0.020	0.087	0.931	7.2e-06
Realism:SS	0.008	0.020	0.403	0.687	1.6e-04
VisualDensity:SS	0.018	0.020	0.899	0.369	7.7e-04
Realism:VD:SS	−0.044	0.028	−1.559	0.119	2.3e-03
HDT			(n = 1089)		
(Intercept)	1.021	0.018	55.755	**<0.001**	1.0e+00
Realism	0.010	0.016	0.595	0.554	5.3e-03
VisualDensity	0.005	0.016	0.301	0.764	8.4e-04
SpatialSize	0.012	0.015	0.775	0.441	8.5e-03
Realism:VD	−0.002	0.019	−0.080	0.937	6.8e-06
Realism:SS	−0.007	0.025	−0.297	0.768	1.6e-03
VisualDensity:SS	0.001	0.019	0.040	0.968	1.6e-06
Realism:VD:SS	−0.004	0.029	−0.135	0.893	1.9e-05
Trail Time			(n=9631)		
(Intercept)	8.957	1.717	5.217	**<0.001**	1.0e-01
SpatialSize	−1.918	2.275	−0.843	0.399	7.4e-05
VisualDensity	0.454	2.275	0.199	0.842	4.1e-06
Realism	−1.386	2.276	−0.609	0.543	3.9e-05
Gain	0.498	1.577	0.316	0.752	1.0e-05
SpatialSize:VD	−2.947	3.217	−0.916	0.360	8.7e-05
SpatialSize:R	−0.811	3.219	−0.252	0.801	6.6e-06
VisualDensity:R	−0.686	3.219	−0.213	0.831	4.7e-06
SpatialSize:G	0.980	2.231	0.439	0.660	2.0e-05
VisualDensity:G	−0.897	2.231	−0.402	0.688	1.7e-05
Realism:G	0.314	2.231	0.141	0.888	2.1e-06
SpatialSize:VD:R	3.343	4.554	0.734	0.463	5.6e-05
SpatialSize:VD:G	3.403	3.154	1.079	0.281	1.2e-04
SpatialSize:R:G	1.950	3.155	0.618	0.537	4.0e-05
VisualDensity:R:G	1.005	3.154	0.319	0.750	1.1e-05
SpatialSize:VD:R:G	−3.142	4.462	−0.704	0.481	5.2e-05
Accuracy			(n = 1376)		
(Intercept)	82.086	2.254	36.413	**<0.001**	9.9e-01
SpatialSize	3.141	1.560	2.013	**0.046**	2.2e-02
VisualDensity	2.606	2.369	1.100	0.321	1.9e-01
Realism	2.558	2.179	1.174	0.282	1.8e-01
SpatialSize:VD	−2.298	2.016	−1.140	0.255	1.0e-03
SpatialSize:R	0.237	2.084	0.114	0.910	1.1e-05
VisualDensity:R	−2.077	2.056	−1.010	0.313	9.8e-04
SpatialSize:VD:R	0.400	2.930	0.136	0.892	2.8e-05

B APPENDIX TABLE 2

Table 5: Temporal variable effects of Day, Session, and Block Models Parameters. Bold values denote the statistical significance of p < 0.05.

Fixed Effect	β	Std. Error	t (n)	$p-value$	$m.r^2$
LDT			(n = 1089)		
(Intercept)	0.924	0.022	42.110	**<0.001**	1.0e+00
Day	0.015	0.005	3.235	**0.001**	9.8e-03
Session	0.013	0.012	1.072	0.284	1.1e-03
Day:Session	−0.013	0.007	−1.951	0.051	3.6e-03
HDT			(n = 1089)		
(Intercept)	1.066	0.014	75.626	**<0.001**	9.9e-01
Day	−0.018	0.005	−3.350	**0.001**	4.9e-02
Session	−0.026	0.014	−1.867	0.063	1.4e-02
Day:Session	0.006	0.007	0.830	0.407	2.9e-03
Trail Time			(n=9631)		
(Intercept)	8.503	2.368	3.590	**<0.001**	1.8e-03
Day	−0.932	1.246	−0.748	0.455	5.8e-05
Session	5.227	3.296	1.586	0.113	2.6e-04
Block	−0.527	0.778	−0.678	0.498	4.8e-05
Gain	2.953	2.285	1.292	0.196	1.7e-04
Day:Ses	−2.965	1.762	−1.683	0.092	3.0e-04
Day:Blo	0.192	0.416	0.461	0.645	2.2e-05
Session:Blo	−0.853	1.100	−0.776	0.438	6.3e-05
Day:G	−0.342	1.222	−0.280	0.780	8.2e-06
Session:G	−5.873	3.232	−1.817	0.069	3.4e-04
Block:G	−0.023	0.763	−0.030	0.976	9.2e-08
Day:Ses:Blo	0.548	0.588	0.932	0.351	9.1e-05
Day:Ses:G	3.267	1.728	1.891	0.059	3.7e-04
Day:Blo:G	−0.003	0.408	−0.007	0.995	4.9e-09
Session:Blo:G	0.927	1.078	0.859	0.390	7.7e-05
Day:Ses:Blo:G	−0.615	0.577	−1.066	0.287	1.2e-04
Accuracy			(n = 1376)		
(Intercept)	79.716	2.326	34.271	**<0.001**	9.9e-01
Day	3.098	0.805	3.846	**<0.001**	1.1e-02
Session	3.097	2.121	1.460	0.144	1.6e-03
Block	0.600	0.499	1.204	0.229	1.1e-03
Day:Ses	−1.372	1.135	−1.209	0.227	1.1e-03
Day:Blo	−0.194	0.266	−0.729	0.466	4.0e-04
Session:Blo	−0.081	0.705	−0.114	0.909	9.8e-06
Day:Ses:Blo	−0.250	0.377	−0.663	0.507	3.3e-04

C LATIN SQUARE SETTING

Participant	Scene Sequence
1 to 4	1, 2, 3, 4, 5, 6, 7, 8
5 to 8	2, 3, 4, 5, 6, 7, 8, 1
9 to 12	3, 4, 5, 6, 7, 8, 1, 2
13 to 16	4, 5, 6, 7, 8, 1, 2, 3
17 to 20	5, 6, 7, 8, 1, 2, 3, 4
21 to 23	6, 7, 8, 1, 2, 3, 4, 5
24 to 26	7, 8, 1, 2, 3, 4, 5, 6
27 to 29	8, 1, 2, 3, 4, 5, 6, 7

D APPENDIX TABLE 4

Table 6: Scene Visual Characteristics Psychometric Parameters.

	PSE		Slope	
	Estimate	95% CI	Estimate	95% CI
Landscape	0.973	[0.966, 0.980]	0.158	[0.150, 0.166]
Room	0.995	[0.988, 1.00]	0.175	[0.167, 0.183]
High Vis	0.982	[0.975, 0.988]	0.168	[0.160, 0.175]
Low Vis	0.985	[0.979, 0.993]	0.166	[0.158, 0.174]
High Real	0.978	[0.971, 0.988]	0.166	[0.158, 0.174]
Low Real	0.990	[0.981, 0.998]	0.167	[0.158, 0.175]

E APPENDIX TABLE 5

Table 7: Day and Session Psychometric Parameters

	PSE		Slope	
	Estimate	95% CI	Estimate	95% CI
Day 1	0.990	[0.979, 1.000]	0.144	[0.135, 0.155]
Day 2	0.991	[0.981, 1.01]	0.144	[0.132, 0.154]
Day 3	0.981	[0.971, 0.993]	0.177	[0.163, 0.187]
Day 4	0.974	[0.964, 0.986]	0.201	[0.187, 0.214]
Session 1	0.992	[0.985, 1.000]	0.172	[0.164, 0.181]
Session 2	0.976	[0.969, 0.984]	0.161	[0.154, 0.171]

Received 20 February 2007; revised 12 March 2009; accepted 5 June 2009